Comments on "Effective Radius of Ice Cloud Particle Populations Derived from Aircraft Probes"

H. GERBER

Gerber Scientific, Reston, Virginia

1. Introduction

In the recent paper by Heymsfield et al. (2006, hereafter H06) I am thanked for being a reviewer of their paper. I was not an American Meteorological Society reviewer of their paper, but instead was a co–principal investigator who, along with some of the H06 authors, participated in the Cirrus Regional Study of Tropical Anvils and Cirrus Layers-Florida Area Cirrus Experiment (CRYSTAL-FACE, hereafter C-F) cumulus field study in 2002. Some of the authors fielded cloud probes and I fielded my cloud-integrating nephelometer (CIN; Gerber et al. 2000; see also Garrett et al. 2003) on the University of North Dakota Citation research aircraft. I was also responsible for calculating and placing in the National Aeronautics and Space Administration (NASA) Ames data archive C-F values of the optical extinction coefficient (σ) and asymmetry parameter (g) measured by this CIN on all Citation flights, as well as values of the effective radius (r_e) of the cloud particles obtained by ratioing the total liquid and solid water measured by the counterflow virtual impactor (CVI; Twohy et al.1997) and the extinction measured by the CIN (the archived data can be found in files EC*.CIT, RE*.CIT, and CV*.CIT online at http://espoarchive. nasa.gov/archive/arcs/crystalf/data/citation). The comments made here are limited to describing the performance and evaluation of this particular CIN used on the Citation, topics that H06 deals with at length.

It was already noticed at the Key West, Florida, field site for the C-F study and reported by Gerber (2003) that there was a factor of ~2 difference in Citation σ measured by the CIN versus σ calculated from particle size distributions measured by the forward spectrometer scattering probe (FSSP) and the 2D-C probes on the Citation. Remarkably, this factor of ~2 was found to be independent of the nature of the particles observed in the various C-F clouds, be they small drops found in warm clouds or ice crystals of various shapes and sizes in the colder clouds. H06 states that this difference is a result of the CIN overestimating σ by a similar factor of 2.5. H06 further states that the agreement between CVI, FSSP, and King hot-wire probe measurements of liquid water content (LWC) on the Citation indicated that the CVI was operating accurately, so that the problem in calculating r_e from the CVI/CIN ratio was the σ measured by the CIN. Clearly, either the CIN was overestimating σ or the CVI was underestimating LWC and ice water content (IWC) to cause this consistent factor of ~2 difference.

To test these conclusions in H06 I take another close look at the C-F microphysics data for several Citation flights that flew through clouds with only liquid water droplets. Here the various probes should give the best agreement with respect to LWC, σ, and r_e, because the additional complexity of ice crystal shape does not enter in. Only three such clouds were found in the data archive; however, they are sufficient to provide new insight on the performance of the probes and the validity of the archived values of r_e. In the following I look at the preliminary microphysical data originally submitted to the NASA Ames data archive as well as the final revised data, conclude if the revised data improved agreement between the probes, discuss potential ice crystal breakup on the CIN thought to be a possibility by H06, describe the calibration of the CIN, and come to some new conclusions as to the validity of the Citation data collected during C-F.

2. Microphysics in C-F liquid water clouds

Table 1 gives the basic description of the three liquid water clouds penetrated by the Citation. The data for

---

Corresponding author address: H. Gerber, Gerber Scientific, 1643 Bentana Way, Reston, VA 20190.
E-mail: hgerber6@comcast.net

TABLE 1. Flight times and conditions for the three cloud passes by the Citation aircraft during the CRYSTAL-FACE study when the clouds consisted only of liquid water drops. Times are seconds after midnight UTC.

Date	Flight begin (s)	Data interval (s)	T (°C)	Aircraft speed (m s^{-1})
9 Jul	64 133	69 686–69 712	−4.1	106
11 Jul	64 797	65 463–65 486	10.3	90
29 Jul	61 058	62 257–62 275	1.5	101

the 9 July cloud were already examined during the C-F field study and provided the first evidence that significant differences existed in the Citation's microphysical data. H06 also describes in detail the LWC portion of the 9 July cloud that was slightly supercooled and thus caused ice to build up on the CIN after about 70 000 s (seconds after midnight UTC). The time interval chosen here for the 9 July penetration contains only droplets measured by the FSSP and no larger drops measured by the 2D-C probe.

Figure 1 shows the LWC measured by the FSSP, CVI, and King probes in the three clouds listed in Table 1. The dashed curves indicate the original FSSP$_o$ (upper curve) and CVI$_o$ (lower curve) data submitted initially to the NASA Ames archive, and other curves in Fig. 1 show the final version of the archived data for the same probes (FSSP$_f$ and CVI$_f$). For the cloud on 29 July no data for CVI$_o$ were found, and the dashed curve corresponds to FSSP$_o$. The reexamination of the CVI and FSSP data resulted in significantly smaller values of LWC than the original values (see Table 2). As shown in Fig. 1 and as noted in H06, CVI$_f$ LWC agrees well with the FSSP$_f$ LWC for 9 July; however, both are smaller than King LWC. This behavior of the probes differs for 11 July where FSSP$_f$ LWC now agrees precisely with the King LWC, and CVI$_f$ LWC is significantly smaller than the LWC measured by the other two probes. More differences occur for 29 July. Given this variability in the LWC measurements it is not possible to claim, as in H06, that these probes were measuring LWC accurately. Further, these results for water droplets do not support the good agreement found in H06 between IWC measured by the 2D-C and CVI probes (see Fig. 8a in H06) in C-F clouds dominated by ice crystals.

Figure 2 shows r_e [r_e (μm) = 1500 LWC (g m^{-3})/σ (km^{-1}) g^{-1} m^3 μm km^{-1}] calculated for the various Citation cloud probes for the cloud time intervals listed in Table 1. As in Fig. 1 the dashed lines represent the original FSSP$_o$ and CVI$_o$ data. As expected, given the agreement found for 9 July between the revised FSSP$_f$ and CVI$_f$ LWC values, the agreement between CVI$_f$/
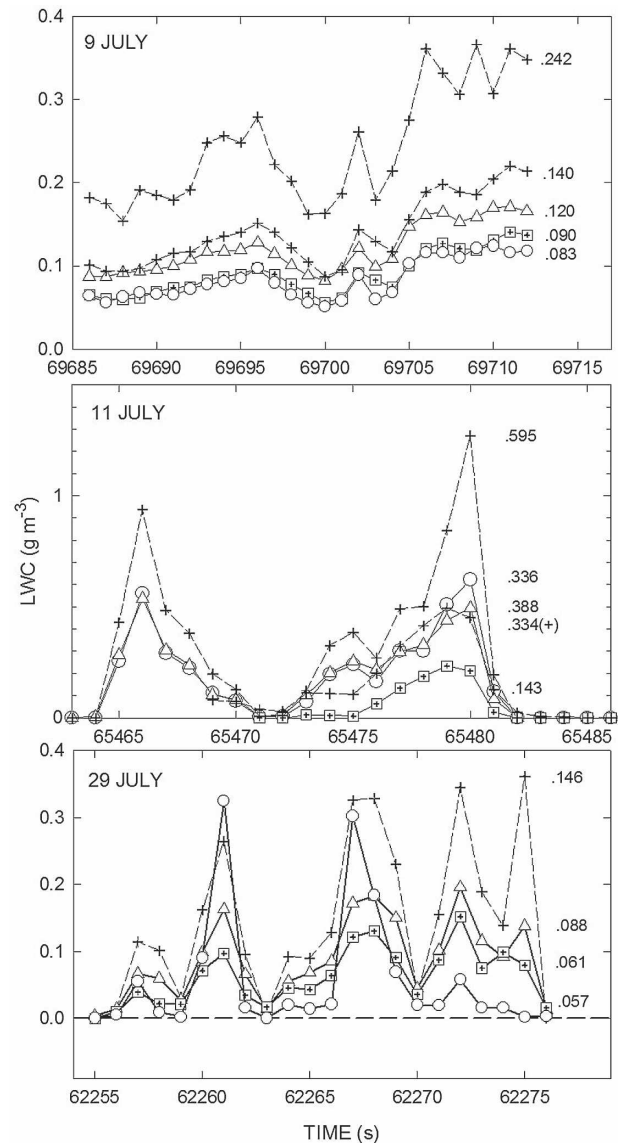

FIG. 1. LWC as a function of time for three cloud probes on the Citation aircraft for penetrations on three days through clouds containing water droplets. The dashed lines represent original data for the CVI$_o$ (upper curve) and the FSSP$_o$ (lower curve), squares are final CVI$_f$ data, circles are final FSSP$_f$ data, and triangles are King hot-wire data. The numbers to the right of the curves are average LWC values for the time intervals shown, and time is in seconds after midnight UTC.

CIN (A) and FSSP$_f$/CIN (C) r_e values is good, but it is no longer so for the other two cloud penetrations (see Table 3). In all three cases CVI$_f$/CIN (A) gives small values of r_e, which should be considered unrealistically small given typical values of r_e found in liquid water clouds. Also, in all three cases r_e from CVI$_f$/CIN (A) is smaller than r_e from King/CIN (E). A direct calculation of r_e (F) from the FSSP$_f$ spectra is also shown in Fig. 2.

TABLE 2. Average LWC for the CVI, FSSP, and King probes on the Citation aircraft for the same time intervals shown in Table 1. The subscript o indicates original data, and the subscript f indicates final archived data.

Date	LWC (g m^{-3})					LWC ratio	
	CVI$_f$	CVI$_o$	FSSP$_f$	FSSP$_o$	King	CVI$_o$/CVI$_f$	FSSP$_o$/FSSP$_f$
9 Jul	0.090	0.140	0.083	0.242	0.120	1.56	2.92
11 Jul	0.143	0.334	0.336	0.595	0.388	2.34	1.77
29 Jul	0.061	———	0.057	0.146	0.088	———	2.56
Average	0.098	0.237	0.159	0.328	0.199	1.95	2.42

This calculation has the advantage of not depending on the potentially large scaling error of the FSSP (e.g., see Baumgardner 1996), but depends only on the relative shape of the FSSP size distribution and an accurate calibration of the size bins of the FSSP. Figure 2 and Table 3 show that the values of r_e from FSSP$_o$/CIN (D) are closest to r_e (F). Except for r_e based on the revised data on 9 July, the values of r_e show significant variability, and using the revised CVI data causes the values of r_e to be reduced to about half of the values of r_e corresponding to the original CVI data.

Figure 3 shows FSSP spectra for the three penetrations listed in Table 1. The arrows indicate the locations for the value of r_e calculated directly from the FSSP spectra (F), as well as locations of r_e calculated from the various ratios of LWC/CIN. Here the close proximity of (D) to (F) is illustrated. However, (D) depends on the original FSSP$_o$ data, while (F) is from the final FSSP$_f$ data. Thus, the agreement between (D) and (F) is not as good as shown, because (F) calculated from the original FSSP$_o$ spectra is about 2 μm larger. H06 concludes that the FSSP was operating properly on the Citation. Yet none of the values of r_e in Fig. 3 calculated from the LWC/σ ratios come close to r_e derived directly from the FSSP spectra, all being too small, with the revised FSSP$_f$ and CVI$_f$ LWC data producing the smallest values of r_e. Again, the unrealistically small values of r_e produced by the CVI/CIN can be a result of the CVI underestimating LWC or the CIN overestimating σ. If the direct measure of r_e from the FSSP$_f$ spectra is considered accurate, a large factor difference of 3.3 exists between those values and r_e from the CVI$_f$/CIN ratio. This is significant because the latter values of r_e are in the file RE*.CIT in the NASA Ames data archive for C–F.

3. Breakup of ice crystals on the leading edge of the CIN

H06 suggests that ice crystals may break up on the leading edge of the CIN prior to passing through the instrument's laser beam causing erroneous values of σ.
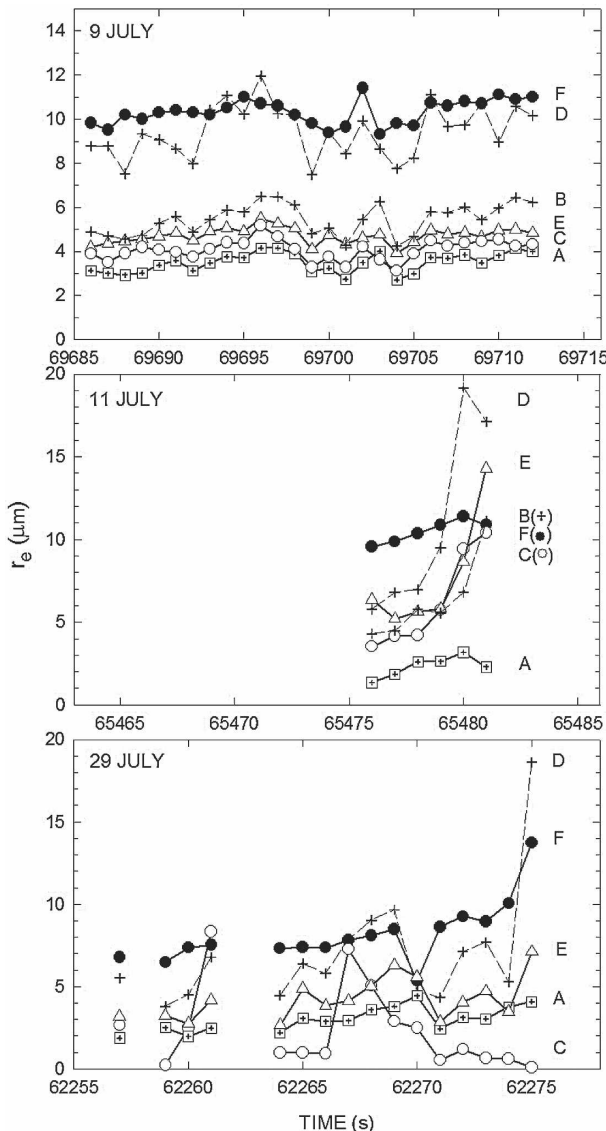

FIG. 2. Effective radius (r_e) as a function of time. Times and symbols are the same as in Fig. 1; letters to the right of the curves are explained in Table 3. The solid circles indicate r_e calculated directly from droplet spectra measured by the FSSP.

TABLE 3. Effective radius r_e (μm) calculated from the ratio of LWC/σ where LWC is measured by the CVI, FSSP, and King probes, and where σ is the extinction coefficient measured by the CIN. The letters A–E indicate which LWC value is used for the ratio, and the letters are used in Figs. 2 and 3 to identify different r_e values. The letter F refers to r_e measured directly from the FSSP droplet spectra.

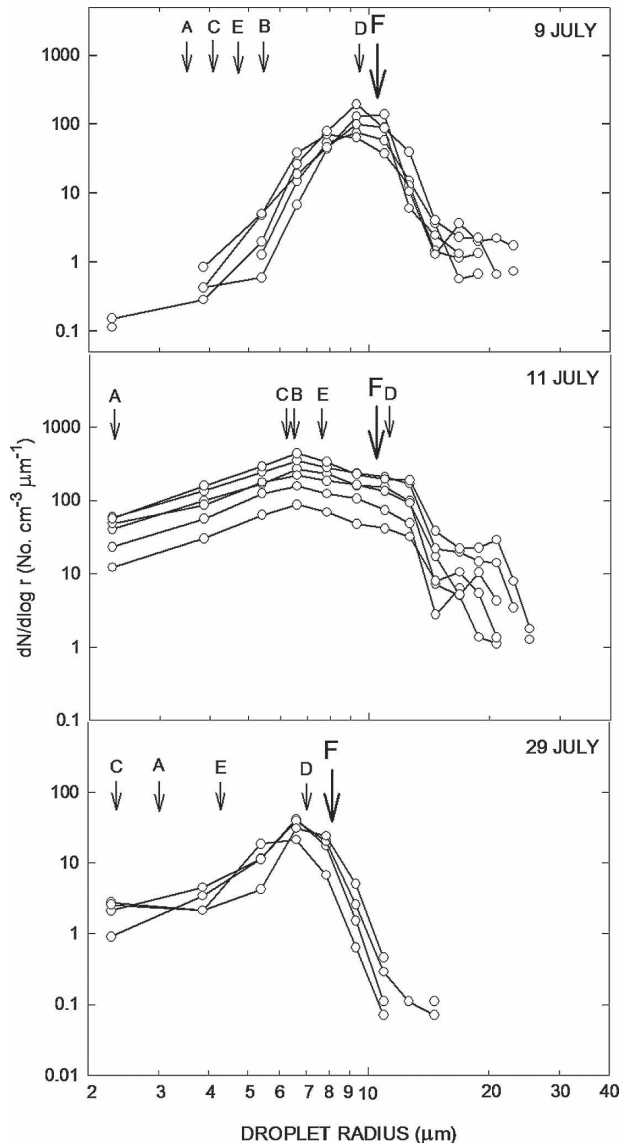| Date	A CVI$_f$/CIN	B CVI$_o$/CIN	C FSSP$_f$/CIN	D FSSP$_o$/CIN	E King/CIN	F FSSP$_f$
9 Jul	3.50	5.45	4.08	9.44	4.72	10.32
11 Jul	2.32	6.34	6.24	10.89	7.66	10.49
29 Jul	3.02	—	2.34	6.98	4.25	8.16
Average	2.95	5.90	4.22	9.10	5.54	9.66

FIG. 3. Droplet size distributions (r = radius) measured by the FSSP for the time intervals shown in Figs. 1 and 2. The bold arrows indicate the average values of effective radius (F) calculated directly from all the FSSP spectra in the intervals, and the other arrows are effective radii calculated from the LWC/σ ratios that are defined in Table 3.

A simple argument to estimate the importance of this possibility is noting that the factor of ~2 difference between σ measured by the particle spectrometer probes (FSSP and 2D-C) and the CIN remained surprisingly constant regardless of the nature of the cloud particles, which ranged from small water drops to larger ice crystals of various sizes and shapes. It would be unexpected that these probes with their large geometrical differences would produce the same contributions from breakup for such a wide variety of cloud particles. Thus, breakup must have been minimal. An exception is an interval on one flight where large snowflake-like agglomerates were observed to cause breakup on the 2D-C (A. Bansemer 2006, personal communication). That situation must have also caused significant breakup on the CIN.

Another way to judge crystal breakup on cloud probes is to look at the crystal images produced by the Cloud Particle Imager (CPI), Spec. Inc., which was also deployed on the Citation during C-F. In that probe obvious breakup would show many shards of ice crystals in the proximity of larger ice crystals that had experienced breakup. Figures 4 and 5 show two CPI images from the Citation of ice crystals that can be considered fragile and thus potentially vulnerable to breakup. Figure 4 shows chainlike aggregates of small primary ice particles found at the highest levels flown by the Citation in a thunderstorm anvil, and Fig. 5 shows a rare case from C-F where the crystals were not highly irregular in shape but instead single bullet rosettes. In both sets of images the criterion for observing breakup from the presence of shards is not met. This result is not unexpected, because ice crystals smaller than about 300–500 μm in diameter are not thought to cause significant breakup on the CPI (A. Korolev 2006, personal communication). The majority of the ice crystals found during C-F were not that large. The fact that the rectangular opening leading to the sensing laser of the CIN is wider than the diameter of the circular opening at the front of the CPI, and that the frontal area per unit length of the rectangular opening of the CIN is
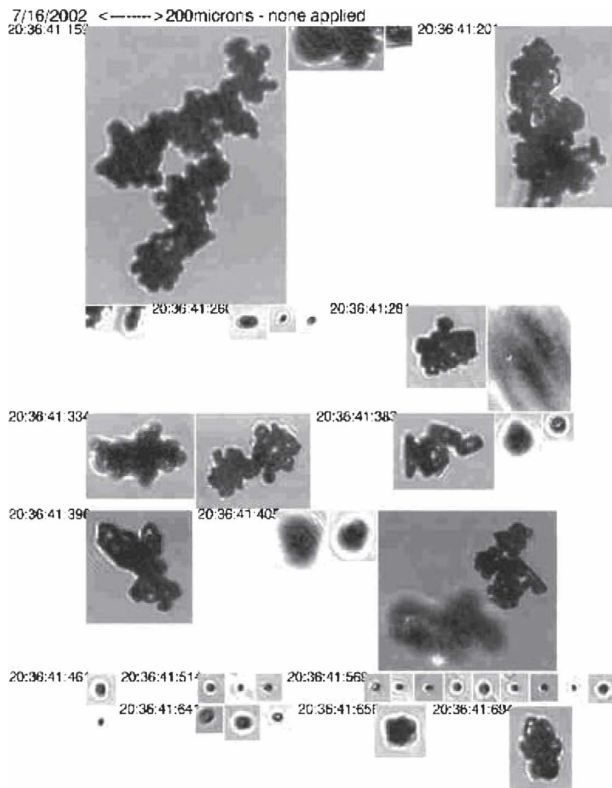
FIG. 4. Example of CPI images of chainlike aggregates of small ice crystals encountered in a thunderstorm anvil. Width of widest image field is 600 μm.
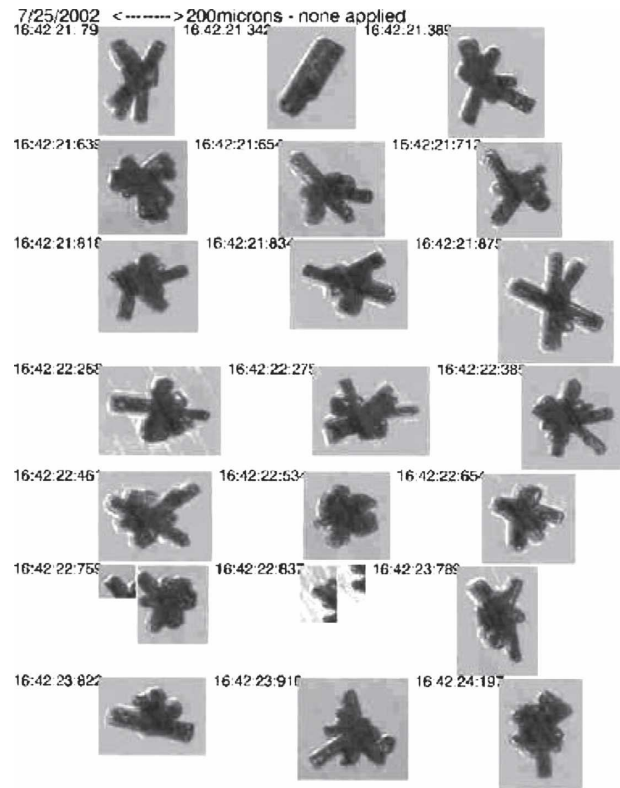

FIG. 5. CPI images of bullet rosettes observed on the 25 Jul 2002 flight of the Citation aircraft. Maximum dimensions of the crystals are about 300 μm.

much smaller than the frontal area of the CPI, suggest that breakup affecting the CIN measurement of σ can be considered minimal.

4. Performance of the CIN

The CIN is a four-detector integrating nephelometer that measures over a range of angles and separates approximately the diffracted light by the particles located in its laser beam from the refracted and reflected light. This permits estimation of σ, g, and the backscatter ratio in the visible spectrum of non-light-absorbing cloud particles covering a wide size range. The principle of operation of the CIN is firmly based on Mie theory, and a full sensitivity analysis for a large variety of ice crystals as well as CIN uncertainty estimates is described in Gerber et al. (2000), and additional evaluation is given in Garrett et al. (2001).

The calibration of the CIN used for the C-F is based on a collocated cloud-chamber comparison between the CIN and a particulate volume monitor (PVM; Gerber et al. 1994). The PVM measures both LWC and particle surface area (PSA), the latter of which is directly related to σ for droplets much greater than the wave-

length of light, and thus can be related to the collocated CIN measurements that are also independent of airspeed. The PSA channel of the PVM was calibrated in the Petten, Netherlands, continuous-flow cloud chamber by comparing it to the total droplet surface area measured by an FSSP for which the size spectrum was scaled to an absolute measure of LWC in the Petten chamber. These calibrations are readily transferred to a field calibration by applying to the CIN a light-diffusing bar, the output of which has been established during the operation of the collocated CIN and PVM in the cloud chamber.

The discovery of the factor of ~2 difference in σ measured by the CIN and the particle spectrometers on the Citation during C-F prompted a postexperiment absolute calibration check of the CIN to establish whether this difference was a result of an incorrect calibration history of the CIN. The approach was to utilize a transmissometer that produces direct measurements of σ, and conduct collocated measurements with the transmissometer and the CIN in clouds. Beer's law is applied to the transmissometer output, and with knowledge of the transmissometer baseline a direct measure of σ is at
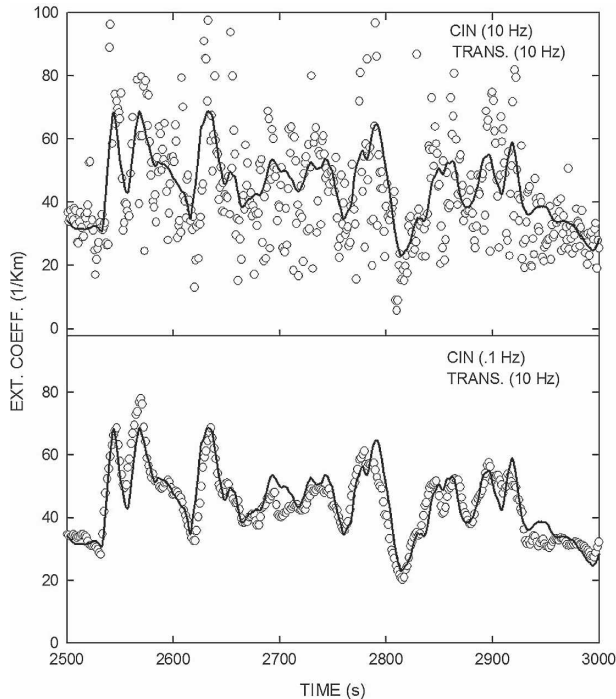
FIG. 6. Comparison of transmissometer (solid curve) and CIN extinction coefficient measurements made in cloud on the summit of Whitetop Mountain, VA, to check the CIN calibration constant. The 10-Hz CIN data has a 100-point running average applied in the lower panel.

hand. Transmissometer measurements have the advantage that they can be done in a relative manner by rationing the light transmitted through the clouds to the light transmitted without the clouds. The collocated intercomparison with CIN and the transmissometer was done on the summit of Whitetop Mountain in southwest Virginia, and is described in Gerber (2004). Figure 6 shows an example of the CIN–transmissometer intercomparison. The top panel shows both instruments recording data at 10 Hz. The large scatter in the CIN data is a result of its baseline being about 100 times smaller than the baseline of the transmissometer, which averages out the small-scale fluctuations of σ in the clouds. The bottom panel shows the same CIN data averaged over 100 data points simulating the integrating effects of the transmissometer. The agreement is good, and it was found that the earlier calibration of the CIN based on the PVM and the Petten chamber work was within 5% of this absolute transmissometer calibration. [See also Garrett (2007), which deals with the comparison of another CIN with an aircraft transmissometer.]

5. Conclusions

A different opinion from that in H06 is reached here on the performance of the microphysics probes used on

the Citation during the C-F study. H06 concludes that the CVI, FSSP, and King probes measured nearly the same LWC on the cloud pass through liquid droplets on 9 July, so these probes must be operating properly. However, it is evident that this conclusion does not hold when data are analyzed from the same probes used on two additional cloud passes in C-F with liquid drops (see Fig. 1 and Table 2). The LWC values in the three liquid water clouds are shown to be inconsistent and vary widely.

The lack of agreement of LWC measured by the cloud probes in the C-F liquid water clouds, even though the droplet spectra fell within the range of these probes, raises doubt on the accuracy of the cloud-probe measurements described in H06 for C-F ice clouds.

H06 argues that, since the FSSP LWC agrees with the LWC measured by the CVI and King probes on 9 July, the CIN must be the source of the factor-of-2.5 difference they found between the extinction coefficients σ measured by the CIN and 2D-C+FSSP. This conclusion is not borne out by the comparison of the LWC probes described here, and the FSSP does not have a reputation of accurately measuring higher moments of droplet spectra.

The CIN used on the Citation was also used previously during other aircraft cloud studies and gave results in agreement with other estimates of σ. For example, during the First International Satellite Cloud Climatology Project (ISCCP) Regional-Arctic Cloud Experiment (FIRE-ACE) study on Arctic clouds, optical thicknesses measured by profiling clouds with the CIN on the University of Washington CV-580 research aircraft gave good agreement with the thicknesses retrieved remotely with the Moderate Resolution Imaging Spectroradiometer (MODIS) instrument on the NASA ER-2 (Platnick et al. 2001). This as well as robust calibrations of this CIN (see Gerber 2004) suggests that the CIN measurements on the Citation were accurate and that the FSSP and 2D-C microphysical data described in H06 and used to calculate σ are suspect.

The contention by H06 that the CIN measures σ too large by a factor of 2.5 strongly affects the values of effective radius (r_e) calculated from the ratio of CVI(IWC)/CIN(σ) by reducing r_e values by the same factor. This results in values of r_e for water-droplet clouds that appear to be unrealistically small, as shown in Fig. 3 and Table 3. These values of r_e are a factor of ~3 smaller than those calculated directly from the FSSP, which is thought by H06 to be operating correctly. I conclude that the final CVI IWC values are too small, rather than the CIN values being too large, and this causes the unrealistically small values of r_e.

The reanalyzed CVI and FSSP final LWC data in the

NASA Ames archive produce no improvement in the calculated values of r_e in comparison to the CVI and FSSP data originally archived. Instead, the reanalyzed data give r_e values with even a greater difference from the direct FSSP-spectra calculation of r_e than the original archived data (see Fig. 3). However, the reduced values of IWC in the reanalyzed CVI data are shown by H06 (see their Fig. 8a) to give good agreement with 2D-C IWC calculations that depend on the Heymsfield et al. (2004) ice crystal density parameterization. I consider this agreement fortuitous.

The values of r_e using the final CVI IWC data and placed in the NASA Ames C-F data archive file RE*.CIT are judged to be much too small. A correction of at least a factor of 2–3 is needed to achieve larger and more realistic values of r_e.

REFERENCES

Baumgardner, D. G., 1996: Status of in-situ microphysical measurements. *Proc. Cloud Modeling and Measurement Workshop,* Boulder, CO, National Oceanic and Atmospheric Administration, 67–102.

Garrett, T. J., 2007: Comments on "Effective radius of ice cloud particle populations derived from aircraft probes." *J. Atmos. Oceanic Technol.,* **24,** 1495–1503.

——, P. V. Hobbs, and H. Gerber, 2001: Shortwave, single-scattering properties of Arctic ice clouds. *J. Geophys. Res.,* **106,** 15 155–15 172.

——, H. Gerber, D. G. Baumgardner, C. H. Twohy, and E. M. Weinstock, 2003: Small, highly reflective ice crystals in low-latitude cirrus. *Geophys. Res. Lett.,* **30,** 2132, doi:10.1029/2003GL018153.

Gerber, H., 2003: Parameterization of the vertical variability of tropical cirrus cloud microphysical and optical properties. Final Rep. NASA Grant NAG5-11618, National Aeronautics and Space Administration, 35 pp.

——, 2004: Accuracy of the cloud integrating nephelometer. Final Rep. NASA Grant NNG04GN43G, National Aeronautics and Space Administration, 18 pp.

——, B. G. Arends, and A. S. Ackerman, 1994: New microphysics sensor for aircraft use. *Atmos. Res.,* **31,** 235–252.

——, V. Takano, T. Garrett, and P. V. Hobbs, 2000: Nephelometer measurements of the asymmetry parameter, volume extinction coefficient, and backscatter ratio in Arctic clouds. *J. Atmos. Sci.,* **57,** 3021–3034.

Heymsfield, A. J., A. Bansemer, C. G. Schmitt, C. Twohy, and M. R. Poellot, 2004: Effective ice particle densities derived from aircraft data. *J. Atmos. Sci.,* **61,** 982–1003.

——, C. Schmitt, A. Bansemer, G. J. van Zadelhoff, M. J. McGill, C. Twohy, and D. Baumgardner, 2006: Effective radius of ice cloud particle populations derived from aircraft probes. *J. Atmos. Oceanic Technol.,* **23,** 361–380.

Platnick, S., J. Y. Li, M. D. King, H. Gerber, and P. V. Hobbs, 2001: A solar reflectance method for retrieving the optical thickness and droplet size of liquid water clouds over snow and ice surfaces. *J. Geophys. Res.,* **106,** 15 185–15 199.

Twohy, C. H., A. J. Schanot, and W. A. Cooper, 1997: Measurement of condensed water content in liquid and ice clouds using an airborne counterflow virtual impactor. *J. Atmos. Oceanic Technol.,* **14,** 197–202.